# Deep-learning prediction of elastic constants for rectangular parallelepiped cubic materials using free-vibration resonant frequencies

Hiroki Fukuda[1†], Akira Nagakubo[1], Oliver Bernard Wright[1,2], Kazuhiro Kyotani[3], and Hirotsugu Ogi[1*] ([1]Grad. School. Eng., Osaka Univ.; [2]Hokkaido Univ.; [3]Insight K. K.)

## 1. Introduction

Elastic constants are important physical quantities in materials science and solid-state physics because they reflect the interatomic potential of materials, and are essential parameters in designing structures. Resonant ultrasound spectroscopy (RUS) has been recognized as a superior method for measuring all independent elastic constants[1–3]. In principle, RUS allows us to determine them in two steps: first, one performs a measurement of a number of free-vibration resonance frequencies of a specimen, and second, one performs an inverse calculation for a set of $C_{ij}$, which reproduces the measured resonant frequencies using the initial guesses of $C_{ij}$. However, obtaining reliable $C_{ij}$ through the inverse calculation relies heavily on initial guesses that are sufficiently close to the true values, which is a very difficult task. In addition, the presence of missing resonant modes in the measurement makes the mode identification in the inverse calculation labyrinthine. Misidentification of the measured and calculated resonance frequencies results in an erroneous convergence of the inverse calculation, which leads to a physically meaningless result.

To overcome these problems, we propose a deep-learning (DL) method for determining the set of $C_{ij}$ without the need for mode identification, and demonstrate its applicability to the class of cubic solids.

## 2. Method

### 2.1 Elasticity images

In this study, we develop a DL scheme specifically for cubic solids. We assume the specimen shape to be a rectangular parallelepiped with a side ratio of 3:4:5. This shape, considered generic in the field, is often used in performing RUS measurements because degeneracy of resonant modes is less likely to occur. A rectangular parallelepiped with sides of length 3, 4 and 5 mm parallel to the cubic crystal axes is taken as a reference specimen.

Our proposed method relies on the creation of elasticity images from resonance frequencies and extracting elastic constant values from them through deep-learning image recognition. We employ the parameter $\tilde{C}$,

$$\tilde{C}_n = \rho f_n^2 \tilde{V}^{2/3} \quad , \tag{1}$$

for the elasticity image construction. Here, $\rho$ and $f_n$ denote the mass density and each free-vibration resonance frequency, respectively, and $n$ denotes the mode number. $\tilde{V}$ is the ratio of the specimen volume under investigation to that of the reference specimen.

To construct the elasticity image, we assume two conditions apply to $\tilde{C}$. First, the range of $\tilde{C}$ is taken from 100 to 13000 TPa/m$^2$. The lower limit (100 TPa/m$^2$) is set because the fundamental frequencies of softer materials give $\tilde{C}$ values close to this value, indicating that it can include the fundamental frequencies of most materials. Second, up to 100 resonant frequencies within the range of $\tilde{C}$ are used for the elasticity image. We divide the range of $\tilde{C}$ values evenly into 900 intervals, and assign binary information in each, indicating the presence or absence of a resonance mode. We convert this one-dimensional data into a three-layer elasticity

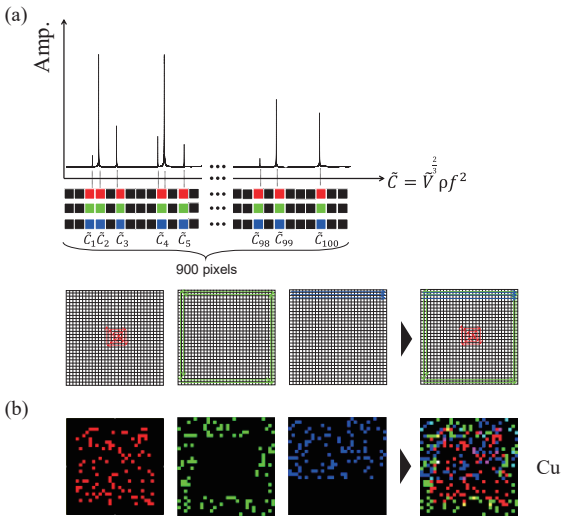


Fig. 1 (a) Construction procedure of the three-layer RGB elasticity image, and (b) the image for the case of Cu.

E-mail : †h.fukuda@qm.prec.eng.osaka-u.ac.jp,
*ogi@prec.eng.osaka-u.ac.jp

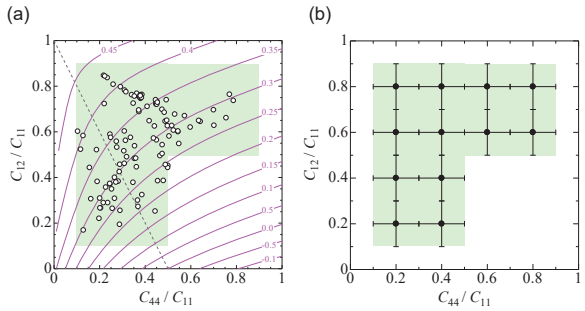


Fig. 2 (a) Blackman diagram for cubic materials. (a) Open circles are reported elastic constants for 110 materials. Red curves indicate the Poisson ratio and the broken line indicates the isotropic material case. We have shaded the datasets area. (b) Solid dots and their error bars denote the areas for each class of dataset for different values of $C_{11}$.

image with $30 \times 30 = 900$ pixels, as shown in Fig. 1 (a). The example of an image corresponding to Cu is shown in Fig. 1 (b).

### 2.2 Dataset preparation and prediction scheme

To prepare the training datasets, we utilize the Blackman diagram to restrict the elastic constant range to be considered. It is known that actual cubic materials lie on the Blackman diagram[4,5], as shown in Fig. 2(a). No natural materials occupy the lower right part in the diagram because this area takes a negative Poisson's ratio. Therefore, only the shaded area is considered for preparing the DL training datasets. We divide the Blackman diagram into 12 classes at each $C_{11}$, as shown in Fig. 2(b). Choosing the value of $C_{11}$ from 50 to 450 GPa in a 25 GPa increments, the total number of classes is 204.

Our scheme consists of two steps. First, an input elasticity image is classified into one of the 204 classes using a pre-trained convolutional neural network. Second, the input elasticity image is fed to a regression network to predict the set of $C_{ij}$ in the vicinity of the classes indicated in the first classification step.

## 3 Results

We first investigated the tolerance of this method to the presence of missing modes for the case of Si with up to 10 missing modes. The predicted values without missing modes are shown in Table I. The accuracy decreases on increasing the number of missing modes. The errors in $C_{11}$, $C_{12}$ and $C_{44}$ with six missing modes are 6, 11 and 2%, respectively, and those with ten missing modes are 8, 11 and 3%, respectively. The prediction accuracy does not differ significantly for the case of six to ten missing modes, even though the dataset did not contain those values, indicating that our method has sufficient stability against missing modes. Our method also exhibits tolerance to dimensional errors: we varied the longest dimension of 5 mm from 0 to 2%, and the predicted value did not change significantly for any choice of dimensional error. These results indicate that our method shows sufficient robustness to errors that could occur in RUS experiments.

Table I Predicted elastic constants $C_{ij}$ (GPa) without missing modes.

| | Predicted values | | | Reported values | | |
|---|---|---|---|---|---|---|
| | $C_{11}$ | $C_{12}$ | $C_{44}$ | $C_{11}$ | $C_{12}$ | $C_{44}$ |
| Al | 116 | 71 | 27 | 113 | 67 | 28 |
| Cr | 348 | 69 | 91 | 350 | 68 | 101 |
| Cu | 177 | 133 | 78 | 168 | 121 | 75 |
| Si | 164 | 63 | 75 | 166 | 64 | 80 |

We investigated the prediction accuracy of this method for 110 real materials with up to 9 missing modes. The prediction error is ~5% for the case of five missing modes. Table I shows the predicted values for Al, Cr, Cu and Si without missing modes.

Finally, we discuss the potential of this cubic method for lower symmetry materials: we also study hexagonal materials, which have five independent elastic constants. Elasticity images of hexagonal materials were substituted into the cubic network and used to predict the sets of cubic $C_{ij}$. Then we converted the output cubic $C_{ij}$ and their original hexagonal $C_{ij}$ to equivalent isotropic values using the Hill approximation and compared them. Both agreed with sufficient accuracy, indicating the applicability of our method to lower symmetry materials.

## 4 Conclusions

In conclusion we propose a method for determining three independent elastic constants of cubic materials using free-vibration resonant frequencies by constructing convolutional neural networks without performing inverse calculations. We convert the resonant frequencies to an elasticity image, and make training datasets within the Blackman diagram. The elasticity image is robust to missing resonant modes and to specimen dimensional errors. The prediction accuracy is examined using 110 existing cubic materials, showing ~5% error or less in the elastic constants. The method can also be applied to determining the average Young's modulus of hexagonal solids, suggesting that our proposed elasticity images faithfully reflect material elastic properties.

## References

1) I. Ohno, Phys. Chem. Miner. **17**, 371 (1990).
2) A. Migliori *et al*., Physica B, **183**, 1 (1993).
3) H. Ogi *et al*., J. Acoust. Soc. Am. **112**, 2553 (2002).
4) M. Blackman, Proc. Roy. Soc. Lond. **164**, 62 (1938).
5) H. Ledbetter *et al*., Phys. Stat. Sol. (b) **245**, 44 (2008).